Bioconjugate Chemistry

Article

pubs.acs.org/bc

Fab-PEG-Fab as a Potential Antibody Mimetic

Hanieh Khalili,[†,‡] Antony Godwin,[§] Ji-won Choi,[§] Rebecca Lever,[†] Peng T. Khaw,[‡] and Steve Brocchini*[,†,‡]

[†]UCL School of Pharmacy, University College London, 29-39 Brunswick Square, London WC1N 1AX, United Kingdom

[‡]NIHR Biomedical Research Centre, Moorfields Eye Hospital and UCL Institute of Ophthalmology, London, EC1 V 9EL, United Kingdom

[§]PolyTherics Ltd, The London Bioscience Innovation Centre, 2 Royal College Street, London NW1 0NH, United Kingdom

Supporting Information

ABSTRACT: IgG antibodies have evolved to be flexible so that they can bind to epitopes located over a wide spatial range. The two Fabs in an IgG antibody are linked together as if each Fab is at the end of a linear, flexible molecule. PEG was used as a scaffold molecule to link two Fabs together to give Fab-PEG-Fab molecules, or FpFs. Preparation of FpFs was achieved with reagents that undergo site-specific conjugation at each PEG terminus by *bis*-alkylation with the two cysteine thiols from a disulfide bond. This allowed each Fab to be conjugated to the PEG scaffold in essentially the same region that each Fab is linked in an IgG. Fabs were sourced directly (e.g., ranibizumab) or monoclonal IgG antibodies were proteolytically digested to obtain the Fabs. This allowed the resulting FpFs to be directly compared to parent IgGs. PEG scaffolds of 6, 10, and 20 kDa were used to make the corresponding FpFs. Dynamic light scatting data suggested the resulting FpFs were similar in size to an IgG antibody and about half the size of a 20 kDa PEGylated-Fab. The solution size of PEG-conjugated proteins is known to be dominated by the extended solution structure of PEG, so it is thought that the smaller size of the FpFs is due to interactions between the two Fabs. Anti-VEGF and anti-Her2 FpFs were prepared and evaluated. The FpFs displayed similar apparent affinities to their parent IgGs. Slower dissociation rates were observed for the anti-VEGF FpFs compared to bevacizumab. The anti-VEGF FpFs also displayed *in vitro* anti-angiogenic properties comparable to or better than bevacizumab. These first studies indicate that FpFs warrant further examination in a therapeutic indication where the presence of the Fc may not be required.

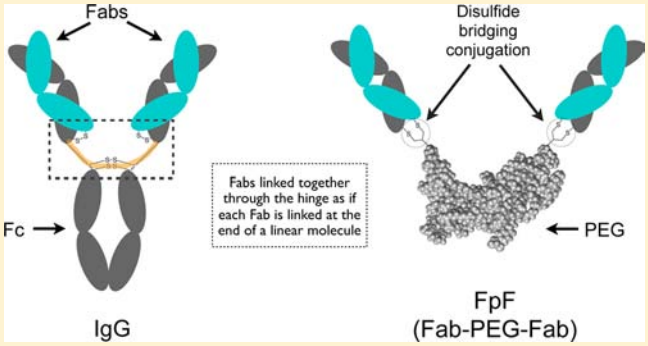

INTRODUCTION

The hinge in IgG antibodies contributes to the flexibility of the two Fabs so they can bind to epitopes located over a wide spatial range.[1−3] Topologically each Fab in an IgG is linked as if the Fabs are on the two ends of a linear molecule (Figure 1a). We hypothesize that conjugating two Fabs at a site near where they are bound to the hinge with an appropriate linking molecule will give bivalent molecules with the binding characteristics of an IgG. We describe a general strategy to use poly(ethylene glycol) (PEG) as a flexible scaffold molecule that, when functionalized as the PEG-di(*bis*-sulfone) **1**, can link two Fabs together to give Fab-PEG-Fab (FpF) (Figure 1a-b) which can act as an IgG mimetic.

Each of the two reactive moieties on the FpF reagent **1** (Figure 1b) are capable of undergoing *bis*-alkylation with the two cysteine thiols that are derived from native disulfides. Analogous reagents capable of *bis*-alkylation on only one terminus have been used to conjugate PEG efficiently to a wide range of proteins including Fabs.[4−6] These reagents were developed to achieve site-specific conjugation while avoiding the need to insert a free cysteine into a protein, which can cause aggregation and disulfide scrambling during protein expression and purification. Mechanistically,[5,7] conjugation is thought to occur by a sequence of addition−elimination reactions (Figure 2) to yield stable thiol ether bonds to rebridge the original protein disulfide bond. The FpF reagent **1** permits the use of Fabs obtained by the proteolytic digestion of intact IgG antibodies (Figure 1a), which allows direct comparison of FpFs with IgGs.

FpFs are being considered for therapeutic applications where only the bivalent binding properties of the two Fabs may be necessary.[8−11] The hinge region in IgG antibodies is also known to be susceptible to cleavage reactions,[12,13] so FpFs are also being developed to be more stable than IgGs. The thiol ether bonds in FpFs are more stable than the corresponding disulfide bond in Fabs, so no light chain dissociation is expected in FpFs. Finally PEG can also decrease the propensity for

Received: May 16, 2013
Revised: September 26, 2013
Published: September 27, 2013

   dx.doi.org/10.1021/bc400246z | *Bioconjugate Chem.* 2013, 24, 1870−1882

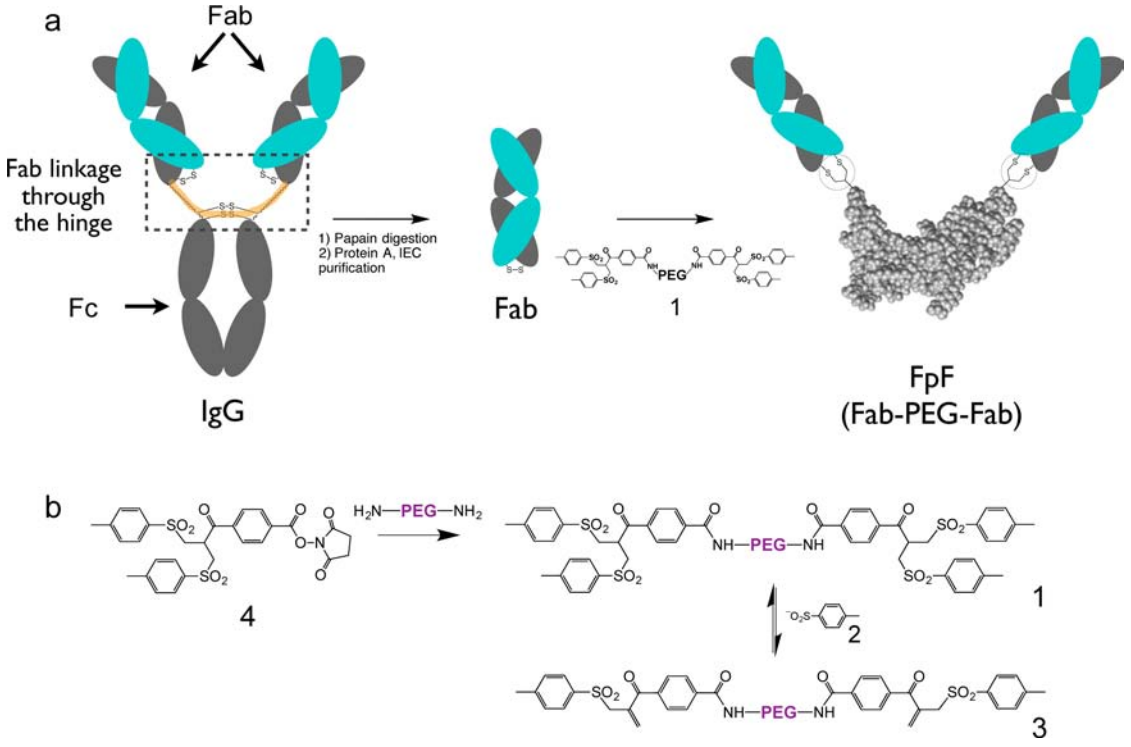

Figure 1. (A) Representation of an IgG showing how the two Fabs topologically are at the two ends of a flexible linear molecule. Also shown is the proteolytic digestion of an IgG to generate its Fab that are then treated with DTT and then linked to each end of a PEG scaffolding molecule using reagent **1** to make an FpF. This strategy allows the properties of an FpP to be directly compared to the starting IgG. (B) Synthesis of FpF reagent **1**. Elimination of toluene sulfinic acid anion **2** yields the reactive FpF reagent **3** which then undergoes reaction with a Fab that had previously been treated with DTT.

aggregation when conjugated to a protein,[14,15] so there may be a lower tendency for aggregation in an FpF than an IgG.

PEG protein conjugates have been used clinically for almost 20 years[16] and several PEGylated proteins have become first line clinical treatments.[17,18] Considering the potential for new ophthalmic treatments based on FpFs, a PEG-aptamer conjugate is registered for clinical intravitreal administration[19] indicating that PEG is safe for intraocular use. Fabs are also known to be safe for intraocular use.[20] The lack of the Fc region in an antibody fragment would reduce the chance for Fc derived side effects.[8−11] Fc receptors within the eye[21] seem to remove antibody therapeutics from the eye.[21−25] There does not appear to be any real increase in local ocular pharmacokinetics due to the presence of an Fc as observed when therapeutic antibodies are used systemically. For example, ranibizumab is a marketed anti-VEGF Fab used to treat ocular indications.[10,20,26] Bevacizumab is a monoclonal IgG1 antibody that also targets VEGF. As expected, bevacizumab has an extended systemic half-life;[27,28] however, the half-life of bevacizumab within the eye after intravitreal injection is comparable to that for ranibizumab.[29−31] FpFs are therefore being examined for potential use as antibody mimetics where there is no need for the presence of the Fc.

Here we describe how bevacizumab was proteolytically digested with papain to give Fab_{beva} that was then used to prepare the corresponding FpF, Fab_{beva}-PEG-Fab_{beva}. This was then compared with the parent antibody, bevacizumab. Ranibizumab (Fab_{rani}) was used directly to prepare the corresponding FpF, Fab_{rani}-PEG-Fab_{rani}. The complementarity determining region (CDR) of ranibizumab has a higher affinity for VEGF than does the corresponding binding region in bevacizumab.[20] Fab_{beva}-PEG-Fab_{beva} and Fab_{rani}-PEG-Fab_{rani} were evaluated by surface plasmon resonance (SPR) and an *in vitro* angiogenesis assay. As a further example of this approach and to examine local ligand binding effects, trastuzumab was proteolytically digested and its Fab (Fab_{trast}) was used to prepare an anti-Her2 FpF, Fab_{trast}-PEG_{20}-Fab_{trast}, which was evaluated by SPR.

EXPERIMENTAL SECTION

Materials. Bevacizumab (Avastin, 25 mg/mL, Genentech) and trastuzumab (Herceptin, 150 mg, Genentech) were purchased commercially. Ranibizumab (Lucentis, 10 mg/mL, Genentech) was obtained from the pooled remaining contents of vials that had been used clinically. Phosphate buffered saline (PBS; 0.16 M NaCl, 0.003 M KCl, 0.008 M Na_2HPO_4, and 0.001 M KH_2PO_4) was prepared with tablets purchased from Oxoid. Acetate buffer A (100 mM sodium acetate, pH 4.0) and acetate buffer B (100 mM sodium acetate, 1 M NaCl, pH 4.0) were prepared for ion-exchange chromatography. Novex bis-tris 4−12% SDS-PAGE gels, Novex Sharp Pre-stained protein standard, NuPAGE MOPS running buffer, NuPAGE LDS sample buffer, and SilverXpress silver staining kit were purchased from Invitrogen. InstantBlue was purchased from Expedeon Ltd. Perchloric acid (0.1 M) and barium chloride (5.0%) solutions for barium iodide staining were prepared in the lab. PD-10 column, cation exchange columns (HiTrap SP HP 1.0 mL) and a Superdex 200 prep grade size exclusion column (34.0 μm particle size) along with Biacore consumables were all purchased from GE Healthcare. Anti-human IgG (Fab specific)-peroxidase, 3,3′,5,5′-tetramethylbenzidine (TMB), and human vascular endothelial growth factor ($hVEGF_{165}$)

dx.doi.org/10.1021/bc400246z | *Bioconjugate Chem.* 2013, 24, 1870−1882

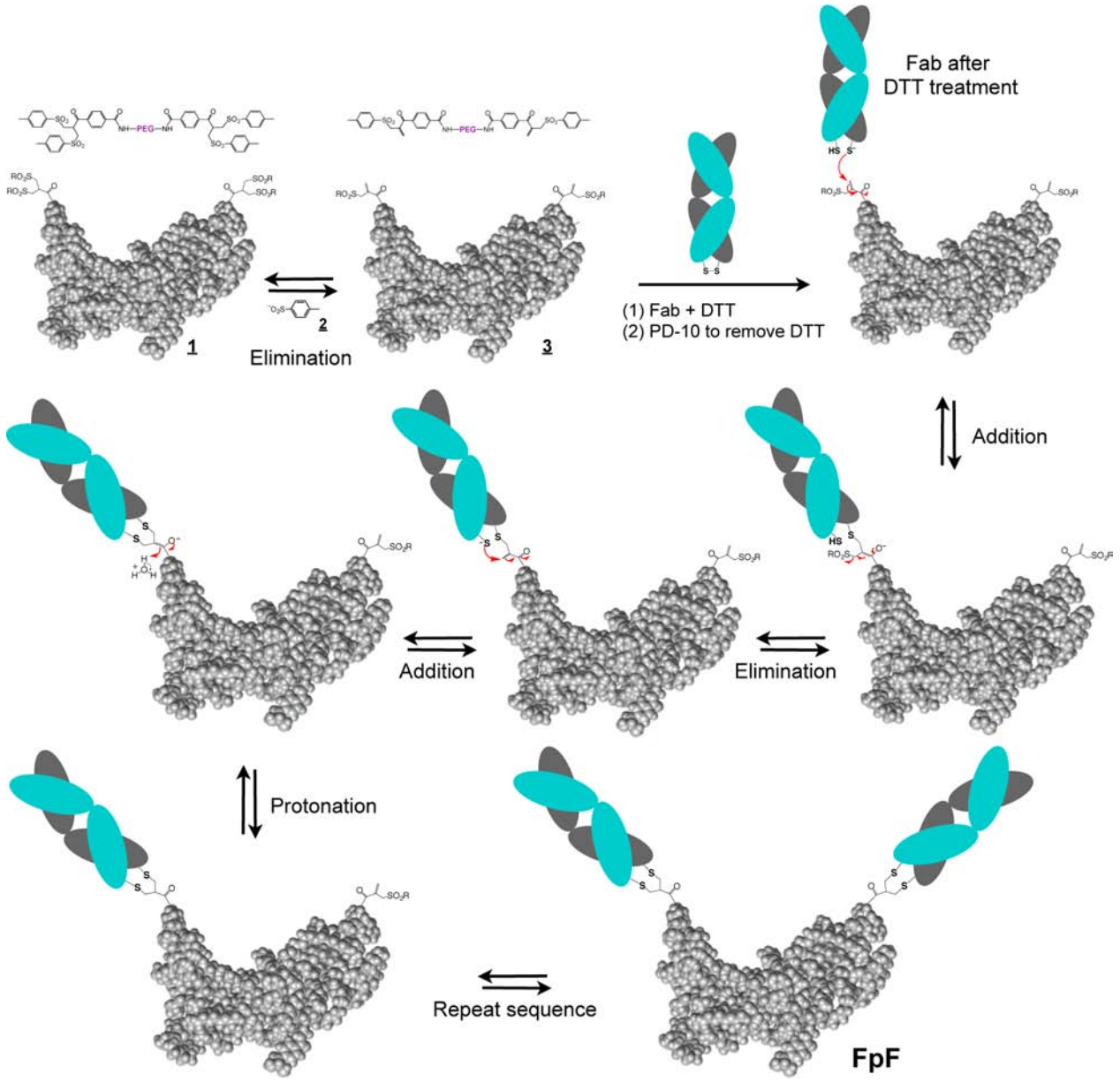

Figure 2. Mechanistically each Fab is thought to form two covalent bonds, one to each cysteine thiol from the Fab disulfide. The conjugation reaction is thought to occur by a sequence of addition and elimination reactions.

were purchased from Sigma-Aldrich. AngioKit human angiogenesis system cultures and media, and AngioSys Image Analysis Software, were purchased from TCS Cellworks Ltd.

Methods. *Preparation of PEG-di(bis-sulfone) 1.* Anhydrous toluene (5 mL), *O,O′*-bis(2-aminoethyl)polyethylene glycol (20 kDa, 100 mg, 0.5×10^{-5} mole, 1 equivalent) and one crystal of 4-dimethylaminopyridine (DMAP) were added to a dry 50 mL Schlenk flask containing a magnetic stir bar. The bottom of the flask was gently heated using a hot air gun until the PEG had fully dissolved. The flask was then allowed to cool to ambient temperature. The stoppered side arm of the Schlenk flask was then connected to a vacuum pump and the flask evacuated to evaporate the toluene. The remaining *O,O′*-bis(2-aminoethyl)polyethylene glycol was dissolved in dichloromethane (5.0 mL), stirred, and to this was added 4-[2,2-bis[(*p*-tolysulfonyl)-methyl] acetyl]benzoic acid-NHS ester **4**[32] (24 mg, 4×10^{-5} mole, 8 equivalents). The reaction mixture was stirred for 48 h at ambient temperature in an argon atmosphere and then the solvent was evaporated using a rotary evaporator. Acetone (5.0 mL) was added and the flask was gently heated until a clear solution was obtained. The reaction flask was then placed in an ice bath for 10 min during which a precipitate began to form. The reaction suspension was centrifuged at 4000 × *g* for 30 min at −10 °C. To maximize the yield of FpF reagent **1**, the acetone centrifugation process was repeated three times. Supernatant was removed and the reagent was dried overnight in a vacuum and then stored under argon at −20 °C.

Proteolytic Digestion of Bevacizumab and Trastuzumab. Isolation of Fab_{beva} and Fab_{trast} by the proteolytic digestion of the corresponding monoclonal antibodies was conducted by routine procedures as previously described.[4] Digestion buffer (20 mM sodium phosphate, 2 mM EDTA, 20 mM cysteine-HCl, pH 7.4) was prepared immediately prior to use. Immobilized 50% papain slurry (1.0 mL) was equilibrated with the digestion buffer. To obtain Fab_{beva}, bevacizumab (12.5

dx.doi.org/10.1021/bc400246z | *Bioconjugate Chem.* 2013, 24, 1870−1882

mg/mL, 1.0 mL) was added to the slurry and the digestion solution was incubated at 37 °C for 5.5 h while being gently shaken at a speed of 250 rpm. After incubation, the solution was separated from the immobilized papain by centrifugation (4000 × *g* for 4 min). The immobilized papain was washed once with the binding buffer (2.0 mL, Tris buffer with EDTA, pH 8.0) and the digestion mixture was eluted over a Protein A column that had been pre-equilibrated with Tris buffer, pH 8.0. The collected fractions were evaluated by SDS-PAGE and the protein concentration was determined by UV spectrometry. Digestion of 12.5 mg of bevacizumab typically gave 5.2−6.4 mg of Fab_{beva} after purification which was approximately a 70% yield.

To obtain $Fab_{trast,}$ a solution of trastuzumab (6.5 mg/mL) was prepared by dilution of 0.5 mL of trastuzumab (12.9 mg/mL) with 0.5 mL of digestion buffer. Trastuzumab was then incubated with pre-equilibrated papain at 37 °C for 20.0 h while being gently shaken at a speed of 250 rpm. The crude Fab was then purified from the digestion mixture by SEC using a mobile phase of PBS (pH 7.3) at a flow rate of 1.0 mL/min.[33] SEC was required to purify Fab_{trast} since this Fab appeared to bind to Protein A. Fab_{trast} was thus obtained in a lower yield (26%) than was possible for Fab_{beva}. The yield for Fab_{trast} may be low due to a susceptibility of trastuzumab to aggregate.[34]

Protein Concentration Determination. A 1.0 mg/mL solution of IgG displays an approximate absorbance of 1.39 at 280 nm with an extinction coefficient of 210,000 M^{-1} cm^{-1}. A Fab fragment at a concentration of 1.0 mg/mL has an absorbance of approximately 1.40 at 280 nm with an extinction coefficient of 216,000 M^{-1} cm^{-1}.[35−38] This latter value was confirmed with a solution of Fab_{rani} (1.0 mg/mL) that was prepared from the pharmaceutical formulation (10 mg/mL). The bicinchoninic acid (BCA) assay was also used to determine protein concentration and to compare with values obtained by UV at 280 nm.[39] As a representative example, a solution of Fab_{beva} was determined to be 0.093 mg/mL by UV spectroscopy and 0.092 mg/mL by BCA assay. As the linker in the PEG reagent contributes to the UV absorbance at 280 nm, BCA assay was used for PEGylated protein samples while UV spectroscopy at 280 nm was used for most unPEGylated protein samples.

Representative Fab PEGylation to Prepare Fab_{beva}-PEG_{20}-Fab_{beva}. Fab_{beva} (2×10^{-5} mmol, 1.0 mL, 1.0 mg/mL in PBS, pH 7.3) was incubated with DTT (1.0 mg) at ambient temperature without shaking for 30 min. DTT was removed by elution over a PD-10 column, and the protein was buffer exchanged into the conjugation buffer (20 mM sodium phosphate, 10 mM EDTA, pH 7.4). PEG-di(*mono*-sulfone) **3** (20 kDa) (1×10^{-5} mmol, 0.06 mL, 3.0 mg/mL in distilled water) was then added to the reduced Fab_{beva} solution (1.0 mg in 3.3 mL). The PEGylation solution was incubated at ambient temperature for approximately 3 h without shaking. Fab_{beva}-PEG_{20}-Fab_{beva} was purified first using a HiTrap Sepharose cation exchange column (IEC-SPHP, 1.0 mL). After sample loading, the column was first eluted with 100% acetate buffer A for 10 min followed by a 30 min linear gradient using 100% acetate buffer B containing 1.0 M NaCl with a flow-rate of 1.0 mL/min. Fractions (1.0 mL) were analyzed by SDS-PAGE and the Fab_{beva}-PEG_{20}-Fab_{beva} was pooled and purified by SEC using a 1.0 mL/min flow rate using PBS, pH 7.4 as mobile phase. The concentration of the purified Fab_{beva}-PEG_{20}-Fab_{beva} was calculated by microBCA assay using Fab_{beva} as a standard. From 1.0 mg of Fab_{beva}, approximately 0.22 mg of purified Fab_{beva}-PEG_{20}-Fab_{beva} was isolated (n = 12).

Comparative Binding Determined by SPR (Biacore). Human recombinant $VEGF_{165}$ (38 kDa) was immobilized on a CM3 chip at an immobilization level of 61 RU using standard carbodiimide-mediated coupling (NHS/EDC, 50/50) and ethanolamine (pH 8.5). Samples were prepared in HBS-EP running buffer (10 mM HEPES, pH 7.4, 150 mM NaCl, 3.0 mM EDTA, 0.005% surfactant P20). All kinetic measurements were conducted at 25 °C at a flow rate of 30 μL/min with an association time of 180 s and dissociation time of 1200 s. Chip regeneration was accomplished by exposure to 10.0 mM glycine−HCl (pH 2.0) for 1200 s. Double-referencing was performed to account for bulk effects caused by changes in the buffer composition or nonspecific binding.[40] Data were evaluated with BIAevaluation software (version 2.1) and the best fit (lowest χ^2) was obtained using a 1:1 binding model. The sensorgram was fitted globally over the association and dissociation phases. Equilibrium dissociation constants (affinity) were calculated from the rate constants ($K_D = k_{off}/k_{on}$).

Comparative Binding Determined by ELISA. Each well in an ELISA plate was incubated with $hVEGF_{165}$ (100 μL, 0.1 μg/mL) overnight at 4 °C. The ligand solution was removed and the blocking buffer (300 μL; PBS with 1% BSA and 0.05% Tween 20) was added into each well and allowed to incubate at ambient temperature for 2 h. Blocking buffer was then aspirated and the wells were washed with PBST (300 μL; PBS with 0.05% Tween 20). Serial dilutions of the test samples in PBS were then added to the wells and the plate was incubated for 2 h at ambient temperature. After removal of the test samples, the wells were washed (300 μL with PBST) three times. Anti-human IgG (Fab specific)-peroxidase (cat. no. Sigma A0293, 100 μL; 1:5000 dilution) was added to each well and allowed to incubate for 1 h at ambient temperature. The wells were aspirated and washed with buffer three times with PBST (300 μL). TMB (100 μL) was then added and color development (blue) was monitored. After approximately 5 min, HCl (50 μL; 1.0 M) was added to each well to stop the reaction and absorbance was measured using a plate reader at 450 nm.

In Vitro Angiogenesis Assay. A HUVEC coculture assay (24-well plate, AngioKit, TCS Cellworks Ltd.) was used according to the manufacturer's instructions. Filter-sterilized (0.22 μm) test samples were diluted in growth medium to their final required concentrations and added to each well (0.5 mL per well) containing a growing culture of HUVEC on the day that the cultures were received. The concentration of $VEGF_{165}$ used was 10 ng/mL in each well and the concentrations of the FpFs were normalized for their protein molecular weights. For example, for molar ratios of 3:1, 1.5:1, and 0.5:1 of sample to VEGF, concentrations of 0.12, 0.06, and 0.02 μg/mL of bevacizumab and 0.08, 0.04, and 0.013 μg/mL of FpFs were required. The samples were preincubated with homodimeric $hVEGF_{165}$ for 2 h at 37 °C before addition to the cells.[41] As negative and positive control, designated wells were treated with medium only (no VEGF) and VEGF (10 ng/mL), respectively. Duplicate wells were prepared for each test environment. The assay plate was then placed in a humidified incubator (37 °C, 5% CO_2). Media was replaced with fresh culture media containing the test samples on days 4, 7, and 9. On day 10, cells were fixed (ice-cold 70% ethanol; 0.5 mL per well). Cells were first exposed to mouse anti-human CD31 primary antibody (1:400 dilution, 0.5 mL per well, 60 min at 37 °C), followed by alkaline phosphatase-linked goat antimouse

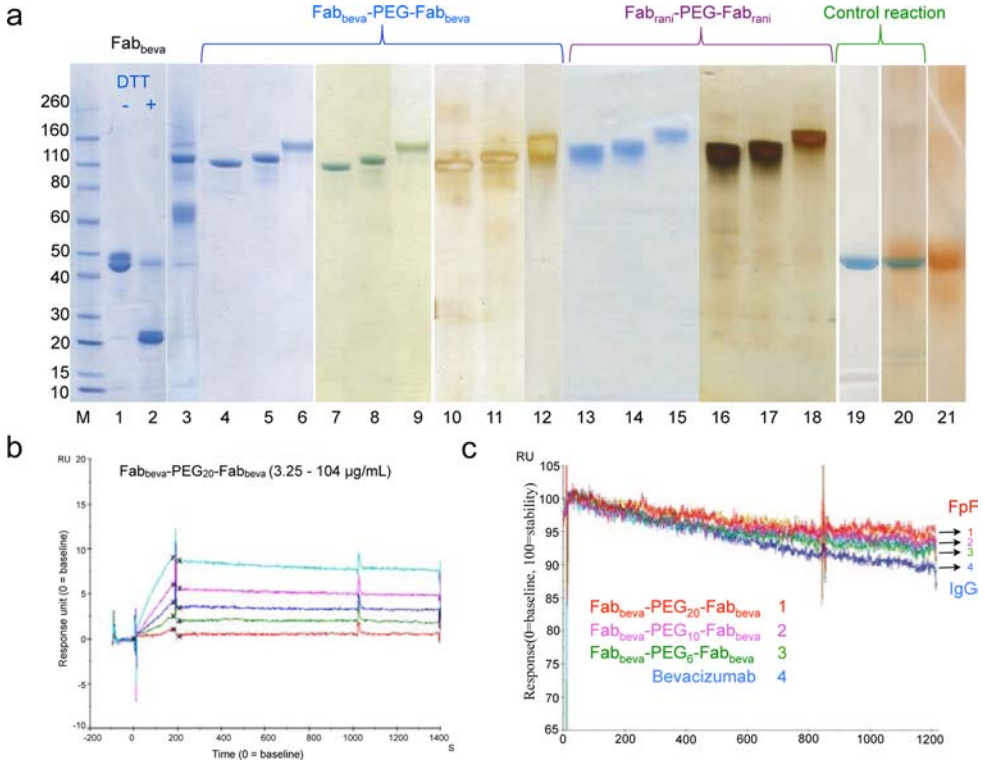

Figure 3. FpF preparation and SPR binding studies. (a) Representative SDS-PAGE gels of FpF preparation and purification. *Lane M*, protein standards (colloidal blue); *Lane 1*, Fab$_{beva}$; *Lane 2*, Fab$_{beva}$ after DTT treatment; *Lane 3*, reaction mixtures for the reaction of Fab$_{beva}$ with 10 kDa FpF reagent **3** (1.0 equiv); *Lanes 4–12*, purified Fab$_{beva}$-PEG-Fab$_{beva}$ (6, 10, 20 kDa PEG) detected with colloidal blue (lanes 4–6), BaI$_2$ for PEG detection (lanes 7–9), and silver stain to establish purity (lanes 10–12); *Lanes 13–18*, purified Fab$_{rani}$-PEG-Fab$_{rani}$ (6, 10, 20 kDa PEG) detected with colloidal blue (lanes 13–15) and silver stain (lanes 16–18); *Lanes 19–20*, control reaction with Fab$_{rani}$ using 20 kDa FpF reagent **3** (1.0 equiv) detected with colloidal blue (lane 19), BaI$_2$ (lane 20); *Lane 21*, FpF reagent **3** (20 kDa) detected with BaI$_2$. (b) Binding sensorgrams for Fab$_{beva}$-PEG$_{20}$-Fab$_{beva}$ using CM5 chip immobilized with VEGF (208 RU). (c) The dissociation rate profile of Fab$_{beva}$-PEG-Fab$_{beva}$ (6, 10, and 20 kDa PEG) and bevacizumab.

secondary antibody (1:500 dilution, 0.5 mL per well, 60 min at 37 °C). To detect the relative number of CD31-expressing (endothelial) cells per well, soluble substrate *p*-nitrophenol phosphate was applied and, following development, aliquots were transferred to a 96-well plate for detection at 405 nm. Cells were then rinsed and permanently stained for CD31 by applying 5-bromo-4-chloro-3-indolylphosphate/nitroblue-tetrazolium salt. Plates were air-dried and photomicrographs were taken using an upright microscope. The images were subsequently analyzed using AngioSys software to calculate the number of junctions and tubules formed in each well.[42]

RESULTS

Preparation of anti-VEGF FpFs. The FpF reagent **1** was prepared from the N-hydroxysuccinimide ester **4** and PEG-diamines of different molecular weights (6, 10, and 20 kDa) (Figure 1b). Reagent **1** is latently reactive and must first undergo elimination of sulfinic acid anion **2** (Figure 1b) so that conjugation can proceed (Figure 2). Although the FpF reagent **1** can be used directly for conjugation, it was pretreated[4] for this study to eliminate sulfinic acid anion **2** to give compound **3**.

Bevacizumab was proteolytically digested with immobilized papain to give Fab$_{beva}$.[4] The purified Fab$_{beva}$ was then incubated with excess dithiothreitol (DTT) and followed by elution over a PD-10 column to remove DTT (Figure 3a, lanes 1–2). Scouting experiments (Figure S1) with the pretreated FpF reagent **1** (10 kDa PEG) indicated that Fab$_{beva}$ was consumed to give the desired Fab$_{beva}$-PEG-Fab$_{beva}$ product (Figure 3a, lane 3). Fab$_{beva}$-PEG-Fab$_{beva}$ analogues were then prepared with 3 different molecular weights of the FpF reagent **1** (6, 10, and 20 kDa). The products are denoted using subscript '*n*' on PEG$_n$ to distinguish the PEG molecular weight that was used, i.e., Fab$_{beva}$-PEG$_{20}$-Fab$_{beva}$ is derived from the Fab from bevacizumab and the 20 kDa PEG version of reagent **1**. No reaction with the FpF reagent **1** (Figure 3a, lanes 19–21) was observed unless the Fab was first incubated with DTT. This is consistent with other PEG *bis*-alkylating reagents that we have developed where no conjugation is observed in these conditions unless there is free thiol present.[4−6]

Purification of the Fab$_{beva}$-PEG-Fab$_{beva}$ products described here was accomplished by ion exchange chromatography (IEC) followed by size exclusion chromatography (SEC) (Figure 3a, lanes 4–12). Elution of Fab$_{beva}$-PEG-Fab$_{beva}$ from IEC generally required higher salt conditions compared to any mono-PEG Fab species. IEC fractions containing the Fab$_{beva}$-PEG-Fab$_{beva}$ product were pooled, concentrated to 2.0 mL using a Vivaspin Centrifugal Concentrator (2 min, 4000 × *g*), and then purified by SEC to give a single band when analyzed by SDS-PAGE as detected by silver stain (Figure 3a, lanes 10–12). Fab$_{rani}$-PEG-Fab$_{rani}$ products were prepared directly from ranibizumab (Fab$_{rani}$) following the same synthesis and purification protocols (Figure 3a, lanes 13–18).

The thiol ether bonds formed during the disulfide rebridging bis-alkylation reaction to make the FpFs are more stable than the original disulfide bond in the Fab.[5−7] Incubating a Fab in

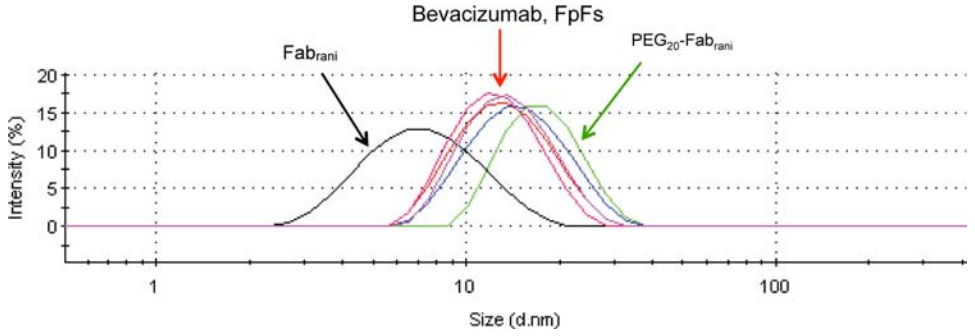

Figure 4. Superposition of DLS traces for Fab$_{rani}$, bevacizumab, and the FpFs derived from 6, 10, and 20 kDa FpF reagent **3**. A PEGylated Fab (PEG$_{20}$-Fab$_{rani}$) is also shown for comparison. DLS measurements were performed three times with each sample.

the presence of DTT causes dissociation of the heavy and light chains (Figure 3a, lane 2). When a FpF was treated with excess DTT no chain dissociation or Fab deconjugation from PEG were observed (Figure S2a, lane 1). The lack of chain dissociation is consistent with both cysteine thiols from the accessible Fab disulfide being conjugated to reagent **1**. The FpFs were not treated with sodium triacetoxyborohydride after conjugation[7] in this study. Storage of the FpF in aqueous buffer (PBS, pH 7.4) at 4 °C for 6 months (Figure S2a, lanes 2−4) also did not appear to cause aggregation or dissociation. In contrast to what was observed for bevacizumab (Figure S2b, lanes 4−6), incubation of Fab$_{rani}$-PEG-Fab$_{rani}$ (Figure S2b, lanes 1−3) at 37 °C (pH 7.4, PBS) for 2 days did not appear to result in chain dissociation or significant aggregation.

Using dynamic light scattering (DLS), the solution size of 20 kDa PEG-Fab (PEG$_{20}$-Fab$_{rani}$; 21.2 ± 1.8 nm) which was derived from a PEGylation reagent with the bis-alkylating moiety used in this study on only one end of the PEG[4,6] is about double that of 10 kDa PEG-Fab conjugate (Fab$_{10}$-Fab$_{rani}$; 10.3 ± 0.6 nm). The solution size of the 20 kDa FpF, Fab$_{rani}$-PEG$_{20}$-Fab$_{rani}$ (11.6 ± 0.2 nm) was about half that of PEG$_{20}$-Fab$_{rani}$ conjugate, but comparable to bevacizumab (12.8 ± 0.2 nm) as were the 6 and 10 kDa FpFs (Figure 4).

Binding Studies with VEGF. The apparent binding affinity (K_D), and the association (k_a) and dissociation rate constants (k_d) of the FpFs were determined by surface plasmon resonance (SPR) (Biacore X-100). VEGF$_{165}$ is a dimer, so there are two binding sites for Fab$_{beva}$.[43] Low-density immobilization of VEGF$_{165}$ (61 RU) and a high flow rate (30 μL/min) were used to minimize mass transfer limitations and rebinding effects over the chip.[44−46] All the anti-VEGF FpFs that were prepared from both Fab$_{beva}$ and Fab$_{rani}$ displayed concentration dependent binding sensorgrams (Figure 3b) with residual plots scattered around zero (Figure S3). The kinetic rate constants and affinities were calculated (Table 1) using a 1:1 binding model resulting in the fitting parameters listed in Table S1.

The apparent K_D values for all of the Fab$_{beva}$-PEG-Fab$_{beva}$ products were similar to those of the parent IgG, bevacizumab (Table 1). Both the association (k_a) and dissociation (k_d) constants tended to be smaller for the Fab$_{beva}$-PEG-Fab$_{beva}$ products compared to bevacizumab. The superposition of the dissociation phase of the sensorgrams[4] illustrates the slower rate of dissociation for Fab$_{beva}$-PEG-Fab$_{beva}$ compared to bevacizumab (Figure 3c). As anticipated,[4] the FpF also displays a considerably slower dissociation rate compared to the monovalent, starting Fab$_{beva}$ (Figure S4).

Table 1. Kinetic Rate Constants and Affinity Values of the Fab$_{beva}$-PEG-Fab$_{beva}$ FpFs as Determined by SPR Using Immobilized VEGF$_{165}$ (CM3 chip, 61 RU)[a]

samples	k_a (×10^4) M^{-1} s^{-1}	k_d (×10^{-5}) s^{-1}	K_D (k_d/k_a) nM
Bevacizumab[b]	6.12	8.16	1.33
Fab$_{beva}$-PEG$_6$-Fab$_{beva}$	3.43	5.29	1.54
Fab$_{beva}$-PEG$_{10}$-Fab$_{beva}$	4.46	5.65	1.27
Fab$_{beva}$-PEG$_{20}$-Fab$_{beva}$	1.96	3.02	1.53
Fab$_{rani}$[b]	3.65	ND	ND
Fab$_{rani}$-PEG$_6$-Fab$_{rani}$	3.80	ND	ND

[a]The range of concentrations used for the Fab-PEG-Fab conjugates and bevacizumab was 0.02 μM to 0.8 μM. Kinetic rate constants could not be determined (ND) for Fab$_{rani}$ and its conjugate. [b]Reported in Khalili et al.[4]

The monovalent ranibizumab (Fab$_{rani}$) did not dissociate when evaluated by SPR at 25 °C (Table 1) during the time allowed for dissociation, which is consistent with previous reports.[43,47,48] Instead, relative apparent binding affinities were determined using an anti-VEGF ELISA. The results indicated that the apparent K_D value for Fab$_{rani}$-PEG$_6$-Fab$_{rani}$ was greater than Fab$_{rani}$ alone and similar to bevacizumab (Figure 5a). The Fab$_{beva}$ FpFs also displayed similar apparent K_D values to bevacizumab (Figure 5b), which was consistent with what was observed by SPR.

Comparative Evaluation of *in Vitro* Inhibition of Angiogenesis. The anti-VEGF FpFs were evaluated using a human umbilical vein endothelial cell (HUVEC) coculture (AngioKit, TCS Cellworks Ltd.). This assay measures the migration and the formation of an anastomosing network characterized by tubule and junction formation during HUVEC proliferation. Inhibition of VEGF-induced HUVEC proliferation has been reported[41] to occur by adding a 2.6:1 molar ratio of bevacizumab to VEGF$_{165}$. The FpFs were evaluated using molar ratios of 3.0, 1.5, and 0.5 to VEGF. To differentiate between the endothelial tubular network and nonendothelial structures of similar apparent morphology, CD31 was used as an endothelial marker to detect the process of angiogenesis based on junction and tubule formation.

Images after staining for CD31 indicated that inhibition of angiogenesis had occurred for all of the FpFs (Figure 6a for Fab$_{rani}$-PEG-Fab$_{rani}$ and Figures S5−6a for Fab$_{beva}$-PEG-Fab$_{beva}$). Quantification of tubule and junction formation (AngioSys Image Analysis Software, TCS Cellworks Ltd.) indicated that the formation of both structures was inhibited in a concentration dependent manner by the anti-VEGF FpFs (Figure 6b and Figure S6b). Both the Fab$_{rani}$ and Fab$_{beva}$

dx.doi.org/10.1021/bc400246z | Bioconjugate Chem. 2013, 24, 1870−1882

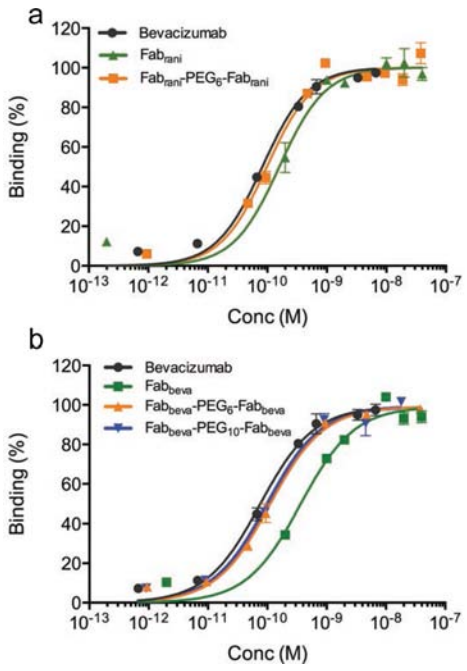

Figure 5. Superimposed ELISA binding saturation curves of (a) Fab$_{rani}$-PEG$_6$-Fab$_{rani}$, Fab$_{rani}$ and bevacizumab, (b) bevacizumab, Fab$_{beva}$ and Fab$_{beva}$-PEG-Fab$_{beva}$ (6, 10 kDa PEG). The anti-VEGF FpFs displayed similar relative apparent affinities with bevacizumab as was observed by SPR.

derived FpFs inhibited angiogenesis *in vitro* better than bevacizumab.

FpF Derived from Fab$_{trast}$. As a second example we elected to evaluate an FpF that was targeted to a cell surface receptor. Trastuzumab is a clinically used IgG antibody that binds to Her2. Analogous to bevacizumab, trastuzumab was proteolytically digested to give Fab$_{trast}$, which was then used to prepare Fab$_{trast}$-PEG$_{20}$-Fab$_{trast}$ (Figure 7). The synthesis and purification of Fab$_{trast}$-PEG$_{20}$-Fab$_{trast}$ (n = 5) was accomplished in the same way as for the anti-VEGF FpFs. Analogous to VEGF, Her2 was also immobilized at low density using a CM3 chip (51 RU). SPR analysis indicated that trastuzumab and Fab$_{trast}$-PEG$_{20}$-Fab$_{trast}$ displayed similar binding properties (Table 2) broadly mirroring the results for Fab$_{beva}$-PEG-Fab$_{beva}$.

DISCUSSION

A key challenge for strategies to link proteins together using a chemical step[49−54] is to achieve site-specific conjugation with high efficiency. The FpF reagent **1** exploits the latent reactivity of the two thiols from the accessible disulfide of a Fab (Figure 2). This results in a bridged product linking the two cysteine thiols through a three-carbon bridge that is more stable than the original disulfide.[4,6] Exploiting the reactivity of the cysteine thiols from a native disulfide avoids the limitations of adding a free unpaired cysteine or a non-native amino acid to the Fab.

The approach described here is essentially a combined recombinant-chemical strategy. In the context of this strategy, the molecule used to link different proteins or protein domains must be (i) nontoxic, (ii) able to preserve the function of each protein, and (iii) capable of site-specific conjugation to each protein. If appropriate chemical-recombinant approaches can be developed, they can be used in a modular way to link easy to prepare monofunctional protein 'precursors' into multifunctional proteins that would be difficult to make by recombinant means alone.

A recombinant only approach to make multifunctional therapeutic proteins requires that a polypeptide sequence must be used to link the two proteins together. Considering fusion proteins which is a successful, clinically proven format,[55−59] there is often an increased propensity for aggregation and enhanced degradation during their development.[60,61] The risk of immunogenicity is always present, so polypeptide linkers must be *both* functional and non-antigenic. Compared to naturally occurring proteins with multiple functions,[62−64] therapeutic fusion proteins, including bispecific antibodies, have not evolved to be together, so optimization of the linking polypeptide between two or more different proteins is required.[65−71] Isolating fusion proteins and bispecifics in sufficient amount and purity during early development is often difficult.[72,73] There are, however, thought to be many therapeutic opportunities for multifunctional proteins.[60,74−76] Many approaches have been described and are continuing to be explored to develop bispecific antibodies (for example, ref 77) and bispecific formats that employ antibody and protein scaffolds.[78] Thinking beyond the FpFs described here, when considering possible multifunctional therapeutic proteins, distinct functional segregation between the two (or more) proteins will probably be necessary. This might best be facilitated with a nonpeptide linker such as PEG as is described here.

Considering FpFs as a model to develop recombinant-chemical strategies, Fabs can be produced from *E. coli* cost-effectively.[79] PEG is used in a wide range of therapeutic and healthcare products.[16] While ligands[80−84] and other proteins engineered with free cysteines[85] have been conjugated to both PEG termini, the work described here is the first to use Fabs directly to form FpF molecules as IgG mimetics. The FpF reagent **1** allows PEG to be used as a scaffold molecule to link two Fabs at essentially the same point that occurs naturally for Fabs in an IgG. The hinge region in IgG antibodies is often considered vulnerable to degradation[13] and disulfide scrambling,[3,9] so FpFs may be more stable than IgGs. Preliminary stability studies of the FpFs, especially when incubated with DTT (Figure S2a, lane 1), show there is no heavy−light chain dissociation during SDS-PAGE that would occur with a full IgG or free Fab in the presence of DTT.

Topologically each Fab in an IgG is linked as if the Fabs are on the two ends of a linear molecule (Figure 1a). As a macromolecule, FpFs may share some of the self-associating characteristics of A-B-A block copolymers[86] where it is known that linear polymers functionalized at both ends can self-associate.[87,88] It is known that the size of PEG-protein conjugates is dominated by the presence of PEG.[89,90] Our DLS measurements were consistent with the solution size of PEG-Fab conjugates being dominated by the molecular weight of the PEG. This can be seen by comparing the solution size of a 20 kDa PEG-Fab conjugate (PEG$_{20}$-Fab$_{rani}$; 21.2 ± 1.8 nm) which was about double that of a 10 kDa PEG-Fab conjugate (Fab$_{10}$-Fab$_{rani}$; 10.3 ± 0.6 nm). In contrast, the solution size of the FpFs derived from the 6, 10, and 20 kDa PEG versions of reagent **1** were all similar to each other and were comparable in size to bevacizumab (Figure 4). Differences in the molecular weight of PEG do not appear to influence the solution size of the FpFs in the same way it does when only one protein is conjugated to PEG (i.e., PEG-Fab).

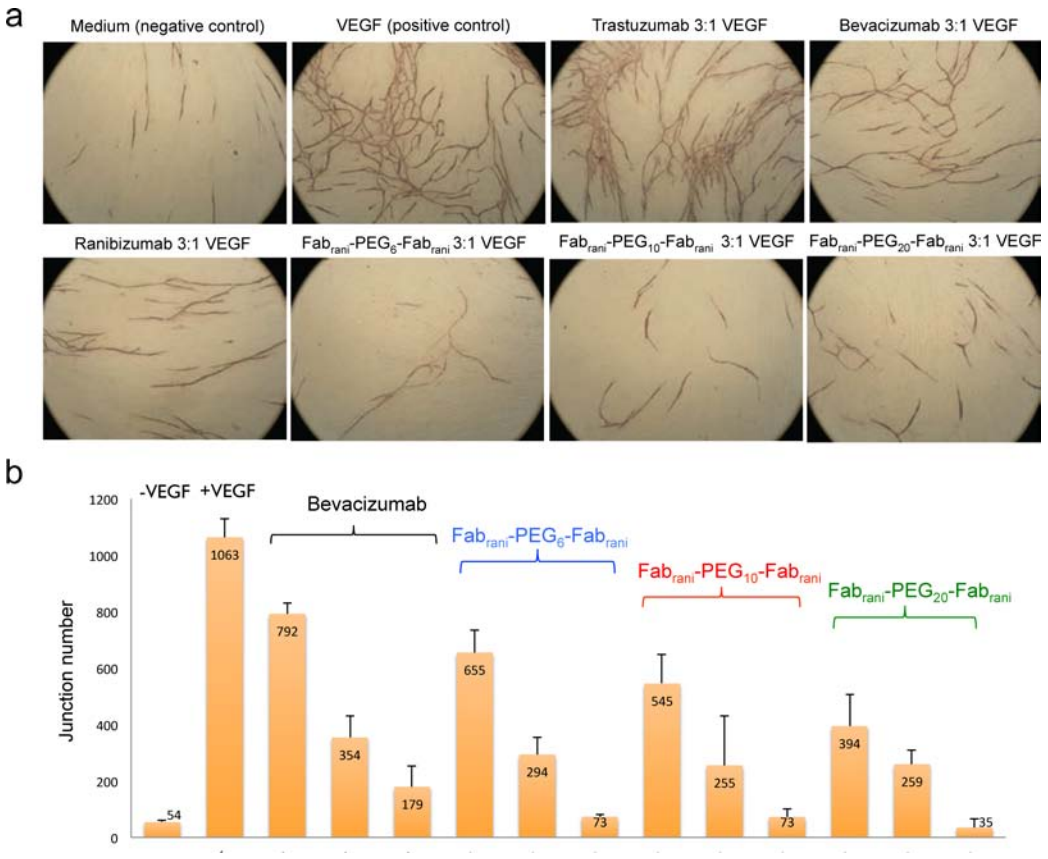

Figure 6. (a) Representative images that were used for AngioSys analysis to quantitate tubule formation using a HUVEC-fibroblast angiogenesis assay. The dark purple structures (tubules) are indicative of angiogenesis and were analyzed to determine the number of junctions. (b) Number of junctions observed for medium alone, medium + VEGF, bevacizumab + VEGF, and Fab$_{rani}$-PEG-Fab$_{rani}$ (6, 10, and 20 kDa) + VEGF. Ratios are the amount of test compound to VEGF. VEGF was present at a fixed concentration of 10 ng/mL. Data are expressed as the mean of two individual cultures per treatment environment.

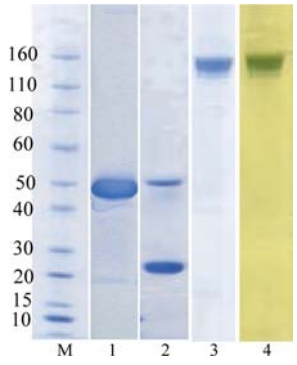

Figure 7. Representative SDS-PAGE gels of the Fab$_{trast}$ and purified Fab$_{trast}$-PEG$_{20}$-Fab$_{trast}$. PEGylation with FpF reagent **3** (20 kDa, 1.0 equiv) was conducted using Fab$_{trast}$ (1.0 mg/mL) after treatment with DTT (1.0 mg/mL). *Lane M*, protein standards (colloidal blue); *Lane 1*, purified Fab$_{trast}$; *Lane 2*, Fab$_{trast}$ treated with DTT; *Lanes 3, 4*, purified Fab$_{trast}$-PEG$_{20}$-Fab$_{trast}$ detected with colloidal blue (lane 3) and BaI$_2$ (lane 4).

Table 2. Kinetic Rate Constants and Affinity Values of the Fab$_{trast}$-PEG-Fab$_{trast}$

samples	k_a ($\times 10^4$) M^{-1} s^{-1}	k_d ($\times 10^{-5}$) s^{-1}	K_D (k_d/k_a) nM
Trastuzumab[a]	38.0	4.2	0.11
Fab$_{trast}$-PEG$_{20}$-Fab$_{trast}$	42.0	5.6	0.13

[a]Reported in Khalili et al.[4]

While antibody dynamics are complex,[91] PEG provided a type of flexibility in the FpFs that may be analogous to the flexibility in the hinge region of IgG antibodies,[1−3] at least to the extent observed here for binding studies. The A-B-A block copolymer motif and the flexibility properties of FpFs may be important to be able to extend a chemical-recombinant strategy to other types of proteins.

The SPR studies indicate that Fab$_{beva}$-PEG-Fab$_{beva}$ displays a similar apparent affinity to bevacizumab (Table 1). The PEG size had little effect on the overall K_D of the FpFs, which indicates PEG sizes of 6 kDa and above confer sufficient flexibility of the two Fab moieties for binding to its target. This may also be indicative that the biological activity can remain broadly independent of PEG molecular weight when conjugation is site-specific.[6]

K_D is the quotient of the dissociation and association rate constants (k_d/k_a), so differences in binding properties between bevacizumab and Fab$_{beva}$-PEG-Fab$_{beva}$ were examined by considering the relative values of k_a and k_d. Overall, the Fab$_{beva}$-PEG-Fab$_{beva}$ FpFs displayed a decreased association rate (k_a) of approximately 40−60% to that observed for bevacizumab (Table 1). In an earlier study, PEGylation reagents that undergo bis-alkylation in the same way as the FpF reagent **1**, but on only one terminus, were used to prepare PEG-Fab$_{beva}$ conjugates. It was found that the k_a of PEG-Fab$_{beva}$ ($\sim 1.0 \times 10^4$ M^{-1} s^{-1}) was about 50% of that observed for Fab$_{beva}$ ($\sim 2 \times 10^4$ M^{-1} s^{-1}).[4] Other studies have shown that most PEGylated proteins reduce k_a to a greater extent (for

dx.doi.org/10.1021/bc400246z | *Bioconjugate Chem.* 2013, 24, 1870−1882

example, refs 92,93), so a reduction of only ~50% in the association rate due to PEG shielding is considered good. The small reduction in the association rate for the FpFs is indicative that the site of conjugation at the accessible disulfide in a Fab is appropriate to minimize PEG shielding effects.

The rate of dissociation (k_d) for the anti-VEGF FpFs was less than bevacizumab. Both VEGF and Her2 ligands were immobilized at very low densities and were spatially well presented. Although there is a rationale for a therapeutic with both anti-VEGF and Her2 binding capacities,[94] in this study we were interested in the differences in the molecular environment of each ligand. In particular, the two binding sites on VEGF were presumably more spatially matched to allow cooperative bivalent binding and local rebinding effects of the FpF within the same immobilized VEGF molecule than Her2. While the relative dissociation constant for Fab_{beva}-PEG_{20}-Fab_{beva} was less than for bevacizumab (Table 1), presumably because of localized rebinding on the dimeric VEGF ligand, the dissociation constant for Fab_{trast}-PEG_{20}-Fab_{trast} was comparable to or slightly faster than that observed for trastuzumab (Table 2) on the monomeric Her2 ligand. Once dissociation occurred, reassociation of the entire Fab_{trast}-PEG-Fab_{trast} molecule was less probable for a ligand with one epitope (Her2) compared to a ligand with 2 epitopes ($VEGF_{165}$). In the case of Fab_{trast}-PEG-Fab_{trast}, the influence of the association rate dominated during any rebinding events, so once unassociated, the rebinding of this FpF was slower than that of the parent IgG.

Exploiting reduced dissociation rates of therapeutics may be a viable strategy to increase efficacy within specific tissues.[95] The slower dissociation of Fab-PEG-Fab compared with that of bevacizumab suggests that once the first Fab_{beva} moiety binds to VEGF, then most of the PEG kinetic (i.e., shielding) and thermodynamic (i.e., entropic[96,97]) costs due to the presence of a flexible PEG have been met. During dissociation when one end of the Fab_{beva}-PEG-Fab_{beva} remains bound to the immobilized VEGF, most of the entropic cost of PEG chain confinement necessary for the second Fab to bind (or rebind) has been paid,[96,98] so reassociation appears to be more favored than with the parent IgG. The conformational flexibility and the low interaction that PEG has with proteins[97] may also enhance the interactions of the Fab moieties in an FpF with the target ligand, especially when one of the Fabs is bound to its target ligand. FpF pharmacokinetics,[99] the location and dynamics of the target,[100] and the specific disease indication[101] will be important properties to evaluate to determine efficacy.

Higher apparent binding affinities were observed by ELISA compared with SPR. This was probably due to (i) more VEGF that was immobilized on the wells of the plate and (ii) longer incubation time of the samples during the ELISA experiment. Both features would be expected to contribute to rebinding effects that would result with increased apparent binding affinities as determined by ELISA. However, the ELISA experiments (Figure 5) suggest that the contribution of bivalency to the apparent affinity in the FpFs was different for two of the precursor Fabs (i.e., Fab_{rani} and Fab_{beva}). There was a greater difference between the starting Fab_{beva} and its corresponding FpF than there was for Fab_{rani} and its corresponding FpF. In both cases, the FpFs appeared to have similar apparent affinity to bevacizumab. The expectation that the FpF for Fab_{rani} would have a higher apparent affinity for VEGF was not borne out by ELISA, probably because of the very high amount of immobilized VEGF and the high affinity of Fab_{rani} and the use of end point analysis within a system that enhances rebinding of a molecule (i.e., Fab_{beva}) with lesser affinity.

The difference between the Fab_{rani} and Fab_{beva} FpFs was discerned by the *in vitro* anti-angiogenesis assay where both FpFs inhibited angiogenesis to what appear a greater extent than bevacizumab (Figure 6; Figures S5−6). There was considerably greater inhibition of angiogenesis by Fab_{rani}-PEG-Fab_{rani} compared to Fab_{beva}-PEG-Fab_{beva}, which is accounted for by the increased affinity of Fab_{rani} compared to Fab_{beva} to VEGF. Increased affinity with decreased dissociation rates might be exploited therapeutically to provide for a longer "therapeutic tail" to decrease dosing frequency.

Dependence of FpF properties on PEG length may also be negligible due to increased flexibility[80,102] of PEG; however, much more study is required and will depend on the Fab-target ligand combination. In some of our *in vitro* anti-angiogenic experiments, low ratios of FpF to VEGF appeared to display a trend with greater inhibition for the ranibizumab FpF made from 20 kDa PEG compared to 6 kDa PEG (Figure 6b). This observation cannot yet be considered to be general and may relate to concentration[103] and interactions between the molecules at the PEG termini as well as to PEG size[104] and to PEG interaction with the target ligand environment.[105] PEG conjugation to proteins does not appear to change biological function,[90,106,107] so once the FpFs are bound to their target, then local rebinding opportunities that can contribute to the binding rate,[108] which in this study were present to a greater extent for VEGF, can be exploited more readily due to where PEG was conjugated to each Fab and to PEG flexibility.

CONCLUSION

We utilized PEG as a scaffold molecule to link two Fabs to prepare anti-VEGF and anti-Her2 FpF molecules as IgG mimetics. A FpF reagent **1** that is capable of bis-alkylation at each end of the PEG allows Fab conjugation in a region near where the Fab is bound to the hinge in an IgG. The absence of an Fc may be appropriate where only receptor antagonism or ligand binding is required[9] and where there is a need to avoid the risk of agonism that can be associated with cross-linking of FcR-expressing cells.[9,10] The binding ability of a semisynthetic molecule (FpF) to mimic a natural, highly evolved molecule (IgG) was to some degree exemplified in the current study. Much work remains to be done to develop FpFs as therapeutics; however, the first steps of (i) employing a site-specific conjugation strategy, (ii) employing molecules known to be safe (e.g., Fabs and PEG), and (iii) maintaining comparative binding and *in vitro* biological properties with the parent IgG have been shown.

ASSOCIATED CONTENT

Supporting Information

Additional data include (i) scouting reactions to prepare FpFs, (ii) SDS-PAGE images for experiments conducted to evaluate the stability of the FpFs, (iii) representative fitting curves and residual plots used in SPR analysis, (iv) comparative dissociation profile of Fab_{beva}-PEG_{20}-Fab_{beva} and Fab_{beva}, (v) representative images of stained cocultures used to evaluate anti-angiogenesis properties of the FpFs derived from bevacizumab, (vi) number of tubules and junctions produced in the HUVEC-based angiogenesis assay that compared bevacizumab and Fab_{beva}-PEG-Fab_{beva}, and (vii) kinetic constants and parameters for Fab_{beva}-PEG-Fab_{beva} and Fab_{rani}-

PEG_6-Fab_{rani} using immobilized VEGF. This material is available free of charge via the Internet at http://pubs.acs.org.

AUTHOR INFORMATION

Corresponding Author

*E-mail: steve.brocchini@ucl.ac.uk.

Notes

The authors declare the following competing financial interest(s): S.B. a full-time academic employee of the UCL School of Pharmacy. S.B. was an academic co-founder of PolyTherics Ltd in 2000 and he has equity in the company. He was a non-paid director/CSO until Dec 2012. He has been a consultant to the company since Jan 2013. Drs Antony Godwin and Ji-won Choi are full-time employees of PolyTherics.

ACKNOWLEDGMENTS

HK gratefully acknowledges funding from the Overseas Research Student Fund and PolyTherics Ltd. H.K., P.T.K., and S.B. are grateful for funding from NIHR Biomedical Research Centre at Moorfields Hospital and the UCL Institute of Ophthalmology, Moorfields Special Trustees, the Helen Hamlyn Trust (in memory of Paul Hamlyn), Fight for Sight and Freemasons Grand Charity, and Dr. Karel Bos and Michael and Ilse Katz Foundation. S.B. is also grateful for funding from the UK Engineering & Physical Sciences Research Council (EPSRC) for the EPSRC Centre for Innovative Manufacturing in Emergent Macromolecular Therapies. Financial support from the consortium of industrial and governmental users for the EPSRC Centre is also acknowledged.

REFERENCES

(1) Paul, W. (2012) *Fundamental Immunology*, pp 140−142, Lippincott Williams and Wilkins.

(2) Harris, L. J., Larson, S. B., Skaletsky, E., and Mcpherson, A. (1998) Comparison of the conformations of two intact monoclonal antibodies with hinges. *Immunol. Rev. 163*, 35−43.

(3) Wang, X., Kumar, S., and Singh, S. (2011) Disulfide scrambling in IgG2monoclonal antibodies: insights from molecular dynamics simulations. *Pharm. Res. 28*, 3128−3143.

(4) Khalili, H., Godwin, A., Choi, J., Lever, R., and Brocchini, S. (2012) Comparative binding of disulfide-bridged PEG-Fabs. *Bioconjugate Chem. 23* (11), 2262−2277.

(5) Balan, S., Choi, J. W., Godwin, A., Teo, I., Laborde, C. M., Heidelberger, S., Zloh, M., Shaunak, S., and Brocchini, S. (2007) Site-specific PEGylation of protein disulfide bonds using a three-carbon bridge. *Bioconjugate Chem. 18* (1), 61−76.

(6) Shaunak, S., Godwin, A., Choi, J. W., Balan, S., Pedone, E., Vijayarangam, D., Heidelberger, S., Teo, I., Zloh, M., and Brocchini, S. (2006) Site-specific PEGylation of native disulfide bonds in therapeutic proteins. *Nat. Chem. Biol.*, 312−313.

(7) Cong, Y., Pawlisz, E., Bryant, P., Balan, S., Laurine, E., Tommasi, R., Singh, R., Dubey, S., Peciak, K., Bird, M., Sivasankar, A., Swierkosz, J., Muroni, M., Heidelberger, S., Farys, M., Khayrzad, F., Edwards, J., Badescu, G., Hodgson, I., Heise, C., Somavarapu, S., Liddell, J., Powell, K., Zloh, M., Choi, J.-W., Godwin, A., and Brocchini, S. (2012) Site-specific PEGylation at histidine tags. *Bioconjugate Chem. 23* (2), 248−263.

(8) Holliger, P., and Hudson, P. J. (2005) Engineered antibody fragments and the rise of single domains. *Nat. Biotechnol. 23* (9), 1126−1136.

(9) Labrijn, A. F., Aalberse, R. C., and Schuurman, J. (2008) When binding is enough: nonactivating antibody formats. *Curr. Opin. Immunol. 20*, 479−485.

(10) Nelson, A. L., and Reichert, J. M. (2009) Development trends for therapeutic antibody fragments. *Nat. Biotechnol. 27* (4), 1−7.

(11) Nelson, A. L. (2010) Antibody fragments; Hope and hype. *mAbs 2* (1), 77−83.

(12) Vlasak, J., and Ionescu, R. (2011) Fragmentation of monoclonal antibodies. *mAbs 3* (3), 253−263.

(13) Yan, B., Boyd, D., Kaschak, T., Tsukuda, J., Shen, A., Lin, Y., Chung, S., Gupta, P., Kamath, A., Wong, A., Vernes, J.-M., Meng, G. Y., Totpal, K., Schaefer, G., Jiang, G., Nogal, B., Emery, C., Vanderlaan, M., Carter, P., Harris, R., and Amanullah, A. (2012) Engineering upper hinge improves stability and effector function of a human IgG1. *J. Biol. Chem. 287* (8), 5891−5897.

(14) Ngadi, N., Abrahamson, J., Fee, C., and Morison, K. (2009) Are PEG molecules a universal protein repellent? *Int. J. Biol. Life Sci. 1* (3), 116−120.

(15) Rajan, R. S., Li, T., Aras, M., Sloey, C., Sutherland, W., Arai, H., Briddell, R., Kinstler, O., Lueras, A. M. K., Zhang, Y., Yeghnazar, H., Treuheit, M., and Brems, D. N. (2006) Modulation of protein aggregation by polyethylene glycol conjugation: GCSF as a case study. *Protein Sci. 15* (5), 1063−1075.

(16) Webster, R., Didier, E., Harris, P., Siegel, N., Stadler, J., Tilbury, L., and Smith, D. (2007) PEGylated proteins:evaluation of their safety in the absence of definitive metabolism studies. *Drug Metab. Dispos. 35* (1), 9−16.

(17) Foster, G. R. (2010) PEGylated interferons for the treatment of chronic hepatitis C: pharmacological and clinical differences between PEGinterferon-2a and PEGinterferon-2b. *Drugs 70* (2), 147−165.

(18) Yang, B. (2006) in *Pharmacokinetics and Pharmacodynamics of Biotech Drugs* (Meibohm, B., Ed.) pp 373−393, Wiley-VCH, Weinheim.

(19) Ng, E. W. M., Shima, D. T., Calias, P., Cunningham, E. T., Guyer, D. R., and Adamis, A. P. (2006) PEGaptanib, a targeted anti-VEGF aptamer for ocular vascular disease. *Nat. Rev. Drug Discovery 5* (2), 123−132.

(20) Meyer, C. H., and Holz, F. G. (2011) Preclinical aspects of anti-VEGF agents for the treatment of wet AMD: ranibizumab and bevacizumab. *Eye 25* (6), 661−672.

(21) Niu, N., Zhang, J., Sun, Y., Wang, S., Sun, Y., Korteweg, C., Gao, W., and Gu, J. (2010) Expression and distribution of immunoglobulin G and its receptors in an immune privileged site: the eye. *Cell. Mol. Life Sci. 68* (14), 2481−2492.

(22) Van Bilsen, K., Van Hagen, P. M., Bastiaans, J., Van Meurs, J. C., Missotten, T., Kuijpers, R. W., Hooijkaas, H., Dingjan, G. M., Baarsma, G. S., and Dik, W. A. (2011) The neonatal Fc receptor is expressed by human retinal pigment epithelial cells and is downregulated by tumour necrosis factor-alpha. *Brit. J. Ophthalmol. 95* (6), 864−868.

(23) Heiduschka, P., Fietz, H., Hofmeister, S., Schultheiss, S., Mack, A. F., Peters, S., Ziemssen, F., Niggemann, B., Julien, S., Bartz-Schmidt, K. U., and Schraermeyer, U. (2007) Penetration of Bevacizumab through the Retina after Intravitreal Injection in the Monkey. *Invest. Ophthalmol. Vis. Sci. 48* (6), 2814−2823.

(24) Kim, H., Robinson, S., and Csaky, K. (2009) FcRn receptor-mediated pharmacokinetics of therapeutic IgG in the eye. *Mol. Vis. 15*, 2803−2812.

(25) Kim, H., Fariss, R. N., Zhang, C., Robinson, S. B., Thill, M., and Csaky, K. G. (2008) Mapping of the neonatal Fc receptor in the rodent eye. *Invest. Ophthalmol. Vis. Sci. 49* (5), 2025−2029.

(26) Bakri, S. J., Snyder, M., Reid, J., Pulido, J., Ezzat, M., and Singh, R. (2007) Pharmacokinetics of intravitreal ranibizumab (Lucentis). *Ophthalmology 114* (12), 2179−2182.

(27) Li, J., Gupta, M., Jin, D., Xin, Y., Visich, J., and Allison, D. E. (2012) Characterization of the long-term pharmacokinetics of bevacizumab following last dose in patients with resected stage II and III carcinoma of the colon. *Cancer Chemother. Pharmacol. 71* (3), 575−580.

(28) Gordon, M. S., Margolin, K., Talpaz, M., Sledge, G. W., Holmgren, E., Benjamin, R., Stalter, S., Shak, S., and Adelman, D. (2001) Phase I safety and pharmacokinetic study of recombinant human anti-vascular endothelial growth factor in patients with advanced cancer. *J. Clin. Oncol. 19* (3), 843−850.

(29) Meyer, C. H., Krohne, T. U., and Holz, F. G. (2011) Intraocular pharmacokinetics after a single intravitreal injection of 1.5 mg versus 3.0 mg of bevacizumab in humans. *Retina (Philadelphia, Pa) 31* (9), 1877−1884.
(30) Krohne, T. U., Liu, Z., Holz, F. G., and Meyer, C. H. (2012) Intraocular pharmacokinetics of ranibizumab following a single intravitreal injection in humans. *Am. J. Ophthal. 154* (4), 682−686.e2.
(31) Xu, L., Lu, T., Tuomi, L., Jumbe, N., Lu, J., Eppler, S., Kuebler, P., Damico-Beyer, L. A., and Joshi, A. (2013) Pharmacokinetics of ranibizumab in patients with neovascular age-related macular degeneration: a population approach. *Invest. Ophthalmol. Vis. Sci. 54* (3), 1616−1624.
(32) Brocchini, S., Balan, S., Godwin, A., Choi, J. W., Zloh, M., and Shaunaik, S. (2006) PEGylation of native disulfide bonds in proteins. *Nat. Protoc. 1* (5), 2241−2252.
(33) Scollard, D. A., Chan, C., Holloway, C. M. B., and Reilly, R. M. (2011) A kit to prepare 111In-DTPA-trastuzumab (Herceptin) Fab fragments injection under GMP conditions for imaging or radioimmunoguided surgery of HER2-positive breast cancer. *Nucl. Med. Biol. 38* (1), 129−136.
(34) Demeule, B., Palais, C., Machaidze, G., Gurny, R., and Arvinte, T. (2009) New methods allowing the detection of protein aggregates, A case study on trastuzumab. *mAbs 1* (2), 142−150.
(35) Barbas, C. F., Crowe, J. E., Cababa, J. R. D., Suzanne, T. M. J., Zebedeei, L., Murphy, B. R., Chanock, R. M., and Burton, D. R. (1992) Human monoclonal Fab fragments derived from a combinatorial library bind to respiratory syncytial virus F glycoprotein and neutralizeinfectivity. *Proc. Natl. Acad. Sci. U.S.A. 89*, 10164−10168.
(36) Minor, L. K. (2006) in *Drug Discovery Series* (Carmen, A., Ed.) p 423, CRC Press, Taylor & Francis Group.
(37) Nikolayenko, I. V., Galkin, O. Y., Grabchenko, N. I., and Spivak, M. Y. (2005) Preparation of highly purified human IgG, IgM, and IgA for immunization and immunoanalysis. *Ukrainica Bioorganica Acta (Ukr. Biokhim. Zh.)*, 3−11.
(38) Thermo Scientific (2008) *Extinction Coefficients guideline:TR0006.3*, pp 1−4.
(39) Kang, J. S., Deluca, P. P., and Lee, K. C. (2009) Emerging PEGylated drugs. *Expert Opin. Emerg. Drugs 14* (2), 363−380.
(40) Myszka, D. G. (1999) Improving biosensor analysis. *J. Mol. Recognit. 12*, 279−284.
(41) Wang, Y., Fei, D., Vanderlaan, M., and Song, A. (2004) Biological activity of bevacizumab, a humanized anti-VEGF antibody in vitro. *Angiogenesis 7* (4), 335−345.
(42) Wang, B., Pearson, T., Manning, G., and Donnelly, R. (2010) In vitro study of thrombin on tubule formation and regulators of angiogenesis. *Clin. Appl. Thromb-Hem. 16* (6), 674−678.
(43) Fuh, G., Wei-Ching, P. W., Mark, L., Chingwei, U., Moffat, V. L., and Wiesmann, C. (2006) Structure-function studies of two synthetic anti-vascular endothelial growth factor fabs and comparison with the Avastin Fab. *J. Biol. Chem. 281* (10), 6625−6631.
(44) Karlsson, R., Hakan Roos, R., Fagerstam, L., and Persson, B. (1994) Kinetic and concentration analysis using BIA technology. *Methods 6*, 99−110.
(45) Schuck, P. (1997) Reliable determination of binding affinity and kinetics using surface plasmon resonance biosensors. *Curr. Opin. Biotechnol. 8*, 498.
(46) Myszka, D. G. (1997) Kinetic analysis of macro molecular interactions using surface plasmon resonance biosensors. *Curr. Opin. Biotechnol. 8*, 50−57.
(47) Chen, Y., Weismann, C., Fun, G., Li, B., Christinger, H. W., Mckay, P., M. De Vos, A., and Lowman, H. B. (1999) Selection and analysis of an optimized anti-VEGF antibody: crystal structure of an affinity-matured Fab in complex with antigen. *J. Mol. Biol. 293*, 865−881.
(48) Lowe, J., Araujo, J., Yang, J., Reich, M., Oldendorp, A., Shiu, V., Quarmby, V., Lowman, H., Lien, S., Gaudreault, J., and Maia, M. (2007) Ranibizumab inhibits multiple forms of biologically active vascular endothelial growth factor in vitro and in vivo. *Exp. Eye Res. 85* (4), 425−430.
(49) Nisonoff, A., and Rivers, M. M. (1961) Recombination of a mixture of univalent antibody fragments of different specificity. *Arch. Biochem. Biophys. 93*, 460−462.
(50) Glennie, M. J., Mcbridg, H. M., Worth, A. T., and Stevenson, G. T. (1987) Preparation and performance of bispecific $F(ab)_2$ antibody containg thioether-linked Fab' fragments. *J Immunol. 139* (7), 2367−2375.
(51) Brennen, M. (1985) Preparation of bispecific antibodies by chemical recombinant of monoclonal immunoglobulin G1 fragments. *Science 229* (4708), 81−83.
(52) Doppalapudi, V. R., Huang, J., Liu, D., Jin, P., Liu, B., Li, L., Desharnais, J., Hagen, C., Levin, N. J., Shields, M. J., Parish, M., Murphy, R. E., Del Rosario, J., Oates, B. D., Lai, J. Y., Matin, M. J., Ainekulu, Z., Bhat, A., Bradshaw, C. W., Woodnutt, G., Lerner, R. A., and Lappe, R. W. (2010) Chemical generation of bispecific antibodies. *Proc. Natl. Acad. Sci. U.S.A. 107* (52), 22611−22616.
(53) Xiao, J., B. S. Hamilton, B. S., and Tolbert, T. J. (2010) Synthetic of N-terminally linked protein and peptide dimers by native chemical ligation. *Bioconjugate Chem. 21*, 1943−1947.
(54) Cao, Y., and Lam, L. (2003) Bispecific antibody conjugates in therapeutics. *Adv. Drug Delivery Rev. 55* (2), 171−197.
(55) Van Assche, G., and Rutgeerts, P. (2000) Anti-TNF agents in Crohn's disease. *Expert Opin. Invest. Drugs 9* (1), 103−111.
(56) Stewart, M. W., Rosenfeld, P. J., Penha, F. M., Wang, F., Yehoshua, Z., Bueno-Lopez, E., and Lopez, P. F. (2012) Pharmacokinetic rationale for dosing every 2 weeks versus 4 weeks with intravitreal ranibizumab, bevacizumab, and aflibercept (vascular endothelial growth factor trap-eye). *Retina 32* (3), 434.
(57) Suzuki, T., Ishii-Watabe, A., Tada, M., Kobayashi, T., Kanayasu-Toyoda, T., Kawanishi, T., and Yamaguchi, T. (2010) Importance of neonatal FcR in regulating the serum half-life of therapeutic proteins containing the Fc domain of human IgG1: a comparative study of the affinity of monoclonal antibodies and Fc-fusion proteins to human neonatal FcR. *J. Immunol. 184* (4), 1968−76.
(58) Korhonen, R., and Moilanen, E. (2009) Abatacept, a novel CD80/86-CD28 T cell co-stimulation modulator, in the treatment of rheumatoid arthritis. *Basic Clin. Pharmacol. Toxicol. 104* (4), 276−84.
(59) Molineux, G. (2011) The development of romiplostim for patients with immune thrombocytopenia. *Ann. N.Y. Acad. Sci. 1222*, 55−63.
(60) Chang, C.-H., Gupta, P., and Goldenberg, D. M. (2009) Advances and challenges in developing cytokine fusion proteins as improved therapeutics. *Expert Opin. Drug Discovery 4* (2), 181−194.
(61) Cordes, A. A., Platt, C. W., Carpenter, J. F., and Randolph, T. W. (2012) Selective domain stabilization as a strategy to reduce fusion protein aggregation. *J. Pharm. Sci. 101* (4), 1400−1409.
(62) Wriggers, W., Chakravarty, S., and Jennings, P. A. (2005) Control of protein functional dynamics by peptide linkers. *Biopolymers 80* (6), 736−746.
(63) Lengyel, J. S., Stott, K. M., Wu, X., Brooks, B. R., Balbo, A., Schuck, P., Perham, R. N., Subramaniam, S., and Milne, J. L. S. (2008) Extended polypeptide linkers establish the spatial architecture of a pyruvate dehydrogenase multienzyme complex. *Structure 16* (1), 93−103.
(64) Ma, B., Tsai, C.-J., Haliloğlu, T., and Nussinov, R. (2011) Dynamic allostery: linkers are not merely flexible. *Structure 19* (7), 907−917.
(65) Gustavsson, M., Lehtiö, J., Denman, S., Teeri, T. T., Hult, K., and Martinelle, M. (2001) Stable linker peptides for a cellulose-binding domain−lipase fusion protein expressed in Pichia pastoris. *Protein Eng. 14* (9), 711−715.
(66) Arai, R., Ueda, H., Kitayama, A., Kamiya, N., and Nagamune, T. (2001) Design of the linkers which effectively separate domains of a bifunctional fusion protein. *Protein Eng. 14* (8), 529−532.
(67) Le Gall, F., Reusch, U., Little, M., and Kipriyanov, S. M. (2004) Effect of linker sequences between the antibody variable domains on the formation, stability and biological activity of a bispecific tandem diabody. *Protein Eng. Des. Sel. 17* (4), 357−366.

(68) Fang, M. (2003) Effects of interlinker sequences on the biological properties of bispecific single-chain antibodies. *Chin. Sci. Bull. 48* (21), 2277.
(69) Zhang, J., Yun, J., Shang, Z., Zhang, X., and Pan, B. (2009) Design and optimization of a linker for fusion protein construction. *Prog. Nat. Sci. 19* (10), 1197−1200.
(70) Chen, X., Lee, H. F., Zaro, J. L., and Shen, W. C. (2011) Effects of receptor binding on plasma half-life of bifunctional transferrin fusion proteins. *Mol. Pharmaceutics 8* (2), 457−465.
(71) Weatherill, E. E., Cain, K. L., Heywood, S. P., Compson, J. E., Heads, J. T., Adams, R., and Humphreys, D. P. (2012) Towards a universal disulphide stabilised single chain Fv format: importance of interchain disulphide bond location and vL-vH orientation. *Protein Eng. Des. Sel. 25* (7), 321−329.
(72) Kufer, P., Lutterbuse, R., and Baeuerle, P. A. (2004) A revival of bispecific antibodies. *Trends Biotechnol. 22* (5), 238−244.
(73) Asano, R., Nakayama, M., Kawaguchi, H., Kubota, T., Nakanishi, T., Umetsu, M., Hayashi, H., Katayose, Y., Unno, M., Kudo, T., and Kumagai, I. (2011) Construction and humanization of a functional bispecific EGFR × CD16 diabody using a refolding system. *FEBS J. 279* (2), 223−233.
(74) Pasche, N., and Neri, D. (2012) Immunocytokines: a novel class of potent armed antibodies. *Drug Discovery Today 17* (11−12), 583−590.
(75) Kontemann, R. (2012) Dual targeting strategies with bispecific antibodies. *mAbs 4* (2), 182−197.
(76) Fischer, N., and Leger, O. (2007) Bispecific antibodies: molecules that enable novel therapeutic strategies. *Pathobiology 74* (1), 3−14.
(77) Strop, P., Ho, W.-H., Boustany, L. M., Abdiche, Y. N., Lindquist, K. C., Farias, S. E., Rickert, M., Appah, C. T., Pascua, E., Radcliffe, T., Sutton, J., Chaparro-Riggers, J., Chen, W., Casas, M. G., Chin, S. M., Wong, O. K., Liu, S.-H., Vergara, G., Shelton, D., Rajpal, A., and Pons, J. (2012) Generating bispecific human IgG1 and IgG2 antibodies from any antibody pair. *J. Mol. Biol. 420* (3), 204−219.
(78) Wurch, T., Pierré, A., and Depil, S. (2012) Novel protein scaffolds as emerging therapeutic proteins: from discovery to clinical proof-of-concept. *Trends Biotechnol. 30* (11), 575−582.
(79) Huang, C.-J., Lin, H., and Yang, X. (2012) Industrial production of recombinant therapeutics in Escherichia coli and its recent advancements. *J. Ind. Microbiol. Biotechnol. 39* (3), 383−399.
(80) Kramer, R. H., and Karpen, J. W. (1998) Spanning binding sites on allosteric proteins with polymer-linked ligand dimers. *Nature 395* (6703), 710−713.
(81) Shan, M., Bujotzek, A., Abendroth, F., Wellner, A., Gust, R., Seitz, O., Weber, M., and Haag, R. (2011) Conformational analysis of bivalent estrogen receptor ligands: from intramolecular to intermolecular binding. *ChemBioChem 12* (17), 2587−2598.
(82) Riley, A. M., Laude, A. J., Taylor, C. W., and Potter, B. V. L (2004) Dimers of D-*myo*-inositol 1,4,5-trisphosphate: design, synthesis, and interaction with ins(1,4,5)P_3 receptors. *Bioconjugate Chem. 15* (2), 278−289.
(83) Das, R., Baird, E., Allen, S., Baird, B., Holowka, D., and Goldstein, B. (2008) Binding mechanisms of PEGylated ligands reveal multiple effects of the PEG scaffold. *Biochemistry 47* (3), 1017−1030.
(84) Stefano, J. E., Bird, J., Kyazike, J., Cheng, A. W.-M., Boudanova, E., Dwyer, M., Hou, L., Qiu, H., Matthews, G., O'callaghan, M., and Pan, C. Q. (2012) High-affinity VEGF antagonists by oligomerization of a minimal sequence VEGF-binding domain. *Bioconjugate Chem. 23* (12), 2354−2364.
(85) Albrecht, H., Denardo, G. L., and Denardo, S. J. (2007) Development of anti-MUC1 di-scFvs for molecular targeting of epithelial cancers, such as breast and prostate cancers. *Q. J. Nucl. Med. Mol. Imaging 51* (4), 304−313.
(86) Lo Verso, F., and Likos, C. N. (2008) End-functionalized polymers: Versatile building blocks for soft materials. *Polymer 49* (6), 1425−1434.
(87) Semenov, A. N., Joanny, J. F., and Khokhlov, A. R. (1995) Associating polymers: equilibrium and linear viscoelasticity. *Macromolecules 28* (4), 1066−1075.
(88) Elli, S., Eusebio, L., Gronchi, P., Ganazzoli, F., and Goisis, M. (2010) Modeling the adsorption behavior of linear end-functionalized poly(ethylene glycol) on an ionic substrate by a coarse-grained Monte Carlo approach. *Langmuir 26* (20), 15814−15823.
(89) Fee, C., and Van Alstine, J. (2004) Prediction of the viscosity radius and the size exclusion chromatography behavior of PEGylated proteins. *Bioconjugate Chem. 15* (6), 1304−1313.
(90) Lu, Y., Harding, S. E., Turner, A., Smith, B., and Athwal, D. S. (2008) Effect of PEGylation on the solution conformation of antibody fragments. *J. Pharm. Sci. 97* (6), 2062−2079.
(91) Thielges, M. C., Zimmermann, J. R., Yu, W., Oda, M., and Romesberg, F. E. (2008) Exploring the energy landscape of antibody−antigen complexes: protein dynamics, flexibility, and molecular recognition. *Biochemistry 47* (27), 7237−7247.
(92) Kubetzko, S., Sarkar, C. A., and Plückthun, A. (2005) Protein PEGylation decreases observed target association rates via a dual blocking mechanism. *Mol. Pharmacol. 68* (5), 1439−1454.
(93) Mabry, R., Rani, M., Geiger, R., Hubbard, G. B., Carrion, R., Brasky, K., Patterson, J. L., Georgiou, G., and Iverson, B. L. (2005) Passive protection against anthrax by using a high-affinity antitoxin antibody fragment lacking an Fc region. *Infect. Immun. 73* (12), 8362−8368.
(94) Bostrom, J., Yu, S.-F., Kan, D., Appleton, B. A., Lee, C. V., Billeci, K., Man, W., Peale, F., Ross, S., Wiesmann, C., and Fuh, G. (2009) Variants of the antibody herceptin that interact with HER2 and VEGF at the antigen binding site. *Science 323* (5921), 1610−1614.
(95) Vauquelin, G., and Charlton, S. J. (2010) Long-lasting target binding and rebinding as mechanisms to prolong in vivo drug action. *Br. J. Pharmacol. 161* (3), 488−508.
(96) Kane, R. S. (2010) Thermodynamics of multivalent interactions: influence of the linker. *Langmuir 26* (11), 8636−8640.
(97) Krishnamurthy, V. M., Semetey, V., Bracher, P. J., Shen, N., and Whitesides, G. M. (2007) Dependence of effective molarity on linker length for an intramolecular protein−ligand system. *J. Am. Chem. Soc. 129* (5), 1312−1320.
(98) Jencks, W. P. (1981) On the attribution and additivity of binding energies. *Proc. Natl. Acad. Sci. U.S.A. 78* (7), 4046−4050.
(99) Vauquelin, G., and Charlton, S. J. (2013) Exploring avidity: understanding the potential gains in functional affinity and target residence time of bivalent and heterobivalent ligands. *Br. J. Pharmacol. 168* (8), 1771−1785.
(100) Copeland, R. A. (2011) Conformational adaptation in drug−target interactions and residence time. *Future Med. Chem. 3* (12), 1491−1501.
(101) Yin, N., Pei, J., and Lai, L. (2013) A comprehensive analysis of the influence of drug binding kinetics on drug action at molecular and systems levels. *Mol. BioSyst. 9* (6), 1381−1389.
(102) Mack, E. T., Snyder, P. W., Perez-Castillejos, R., Bilgiçer, B., Moustakas, D. T., Butte, M. J., and Whitesides, G. M. (2012) Dependence of avidity on linker length for a bivalent ligand−bivalent receptor model system. *J. Am. Chem. Soc. 134* (1), 333−345.
(103) Shewmake, T. A., Solis, F. J., Gillies, R. J., and Caplan, M. R. (2008) Effects of linker length and flexibility on multivalent targeting. *Biomacromolecules 9* (11), 3057−3064.
(104) Cojocariu, G., and Natansohn, A. (2002) Intramolecular complexation in aqueous solutions of an end-capped poly(ethylene glycol). *J. Phys. Chem. B 106* (45), 11737−11745.
(105) Numata, J., Juneja, A., Diestler, D. J., and Knapp, E. W. (2012) Influence of spacer−receptor interactions on the stability of bivalent ligand−receptor complexes. *J. Phys. Chem. B 116* (8), 2595−2604.
(106) Rodríguez-Martínez, J., Solá, R., Castillo, B., Cintrón-Colón, H., Rivera-Rivera, I., Barletta, G., and Griebenow, K. (2008) Stabilization of α-chymotrypsin upon PEGylation correlates with reduced structural dynamics. *Biotechnol. Bioeng. 101* (6), 1142−1149.

(107) Gonnelli, M., and Strambini, G. B. (2009) No effect of covalently linked poly (ethylene glycol) chains on protein internal dynamics. *BBA-Proteins and Proteomics 1794*, 569−576.
(108) Weber, M., Bujotzek, A., and Haag, R. (2012) Quantifying the rebinding effect in multivalent chemical ligand-receptor systems. *J. Chem. Phys. 137* (5), 054111.